Gebeyehu, Esubalew Kasaw; Tarhini, Ali Amin; Tehrani-Bagha, Ali Reza

An ecofriendly approach for hydrophobization of cellulosic nonwovens: A comparative study of different biobased agents

Published in:
Colloids and Surfaces A: Physicochemical and Engineering Aspects

DOI:
10.1016/j.colsurfa.2024.135127

Published: 20/11/2024

Document Version
Publisher's PDF, also known as Version of record

Colloids and Surfaces A: Physicochemical and Engineering Aspects 703 (2024) 135127

Contents lists available at ScienceDirect

Colloids and Surfaces A: Physicochemical and Engineering Aspects

journal homepage: www.elsevier.com/locate/colsurfa

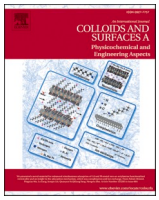

An ecofriendly approach for hydrophobization of cellulosic nonwovens: A comparative study of different biobased agents

Esubalew Kasaw Gebeyehu, Ali Amin Tarhini, Ali Reza Tehrani-Bagha *

Department of Bioproducts and Biosystems, School of Chemical Engineering, Aalto University, Vuorimiehentie 1, Espoo 02150, Finland

GRAPHICAL ABSTRACT

Graphical representation of hydrophobic nonwoven material treated with biobased agents, highlighting enhanced water repellency. Generated using Adobe Firefly.

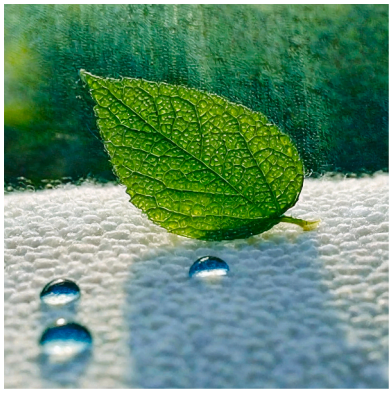

ARTICLE INFO

Keywords:
Hydrophobization
Eco-friendly treatment
Biobased nonwovens
Surface properties
Physio-mechanical properties
Comparative study

ABSTRACT

The purpose of this research was to render hydrophobicity on three different cellulosic nonwovens (NW) using green biobased materials including betulin (Bt), stearic acid (SA), ethyl cellulose (EC), and beeswax (BW). A commercially available Alkyl ketene dimer-based hydrophobizing agent (AKD) was also used for benchmarking. A comparative analysis and comprehensive characterization of the coated samples was conducted using various analytical techniques, including scanning electron microscope (SEM), Fourier transform infrared (FTIR), capillary flow porometry, optical tensiometry, and tensile testing. The treatment of NW materials with selected biobased agents significantly enhanced their hydrophobicity. A water-absorbing air-laid NW1 became hydrophobic after functionalization with Bt achieving the highest water contact angle (WCA) of 134° compared with other biobased agents. To achieve complete hydrophobization of NW2 and NW3, which have larger pore sizes, mixtures of EC with SA and EC with Bt were applied, resulting in WCAs greater than 109°. The SEM micrographs of the coated NW2 and NW3 samples revealed that Bt and SA induced microroughness on the coating surface, with specific portions protruding outward over EC. The treatments did not significantly affect the porosity and tensile strength of the nonwovens, except for AKD and SA treated samples.

* Corresponding author.
E-mail address: ali.tehrani@aalto.fi (A.R. Tehrani-Bagha).

https://doi.org/10.1016/j.colsurfa.2024.135127
Received 27 April 2024; Received in revised form 12 August 2024; Accepted 17 August 2024
Available online 23 August 2024

1. Introduction

Textiles have received much attention in recent decades as a result of their renewed use in other sectors such as construction, transportation, agriculture, medical, and environmental protection [1,2]. Nonwoven fabrics, in particular, address performance requirements in a wide range of applications [3]. The versatility, porosity, permeability, and simplicity of fabrication make nonwovens ideal for technical applications like masks, surgical gowns, filtration systems, and so on. Among the key advantages of nonwoven fabric manufacturing is that it is typically done in a continuous, linked process in which raw materials are first converted into a web and then a finished fabric. Hence, systematic inventions have evolved to meet the requirements of various industries. The desirable properties for specific purposes are imparted through textile finishing. Hydrophobic finishing of cellulosic textile material has attracted increasing attention from academia and manufacturers owing to their practical applications [1] for oil and waterproofing [4,5], anti-fouling [6,7], anti-contamination [8], stain and soil-resistant finish [9], for plastic replacement [10], anti-sticking [10,11], and self-cleaning [12–14].

Cellulose is an abundant natural polymer used in a range of textile applications due to its renewability, substantial strength, breathability, biodegradability, and wearing comfort [15]. Ascribable to the presence of hydroxyl groups in the structure, the porous and rough surface morphology of the fabric, and the capillary action of the fibers, cellulose is hygroscopic and hydrophilic allowing water to be absorbed and spread across its surface [10]. Despite its innate hydrophilicity, cellulose has unrivaled benefits as a hydrophobic textile. The hydrophilicity of cellulose is characterized by the water contact angle which ranges between 0° and 47°. A hydrophobic cotton surface has a water contact angle greater than 90° [10]. To meet the need for water repellency in cellulosic textiles, various finishes with pros and cons are available on the market [10,13,16]. Textile finishes modify the material's interface through two main mechanisms: increasing the roughness and lowering the surface free energy. The free energy at the material's interface causes adhesive interactions between it and the water. When the internal cohesive interactions within the water are stronger than the external adhesive interactions between the water and interface, the water beads up causing the material to repel water. Alternatively, the roughness of the material can skew water's preference for breaking its surface tension to adhere to the substrate.

Common practices for roughening the surface include sizing, applying microparticle coatings, and etching while low surface free energy is achieved with water repellent and polymeric coatings [17,18]. These structural properties on cellulosic surfaces have been produced using a variety of methods as reviewed by [10,18,19] such as electro-spinning [20], polymerization processes, chemical deposition [21], laser deposition, dip-coating, layer-by-layer coating, spray coating, grafting, and plasma processing.

The first method to develop a hydrophobic, cellulosic surface was by mechanical incorporation of the water-repellent products of paraffin emulsions in the fiber pores, in or on the fiber and fabric surface, and in the spacing between the fibers and the yarns [22,23]. Despite being inexpensive and producing uniform effects, the use of these treatments was hindered by their lack of durability to washing and dry cleaning and low breathability. In practice, hydrophobicity on cotton textiles is typically achieved with coatings like rubber, polyvinyl chloride, and polyurethane which also cause a stiff hand, lack of vapor and air permeability, and consequently have poor wear comfort [24,25]. Bonding of the hydrophobic chemicals with cellulosic fiber surface is another strategy. Fatty acid resins are an illustration of this process [25,26]. However, such repellents like stearic acid–melamine released formaldehyde and resulted in a reduction in fabric strength and shade change on colored fabric [27]. Another strategy for a high degree of repellency is forming a repellent film on the surface of a substrate with silicone and fluorocarbon products [28]. Silicone repellents are netted with reasonable durability for washing and enhance seam slippage and pilling. However, careful formulation is required in using silicone repellants as it reduces hydrophobicity if excessive amounts are used. Perhaps, silicone offers no oil and soil repellency and promotes the attraction of hydrophobic dirt. Moreover, residual baths and the effluent of these finish application processes are harmful to aquatic life and silicon-based alternatives are under discussion for their safety profiles. Per- and poly-fluoroalkyl substances (PFAS) give the lowest surface energies of all the repellent finishes in use to make cellulose hydrophobic. However, PFAS change colors during washing, have high costs, contain hazardous aerosols, and their application process requires intensive wastewater treatment. Further, due to its resistance to degradation, long-range mobility, bioaccumulation, and toxicity, PFAS are restricted from use in Europe under the registration, evaluation, authorization, and restriction of chemicals (REACH) framework.

Following a restriction on the use of per- and polyfluoroalkyl compounds, many attempts have been made to render cellulose hydrophobic using fluorocarbon-free chemicals. Despite the available alternatives, PFAS substitutes still face challenges in ensuring effective coverage with smaller quantities, achieving long-lasting durability, maintaining optimal coating thickness, and guaranteeing safety for humans and the environment. Establishing a balance between hydrophobic performance, environmental impact, and while maintaining inherent fabric properties is still challenging. Considering these factors, this study aims to illustrate the effect of hydrophobic treatments on base substrate qualities using environmentally friendly and sustainable hydrophobizing agents. This paper compares the impact of various biobased hydrophobizing agents on the physio-mechanical properties of nonwoven textiles. We discuss how the structure of the nonwoven material, as well as the surface morphology of the coating, correlate with the realized hydrophobicity.

2. Materials and methods

2.1. Materials

A. Fabric

In this study, we used three distinct cellulosic nonwoven materials. NW1, an air-laid nonwoven, was procured from SharpCell Oy - Finland. It consisted of 85% fluff pulp and 15% polymeric binder, with a basis weight of 51.56 g/m^2 and a thickness of 224 μm. NW2 and NW3 were procured from Suominen Oyj - Finland. NW2 was exclusively fabricated from lyocell, boasting a basis weight of 58.21 g/m^2 and a thickness of 260 μm. NW3 was a composite material combining 80-85% cellulose and 15-20% PLA, featuring a basis weight of 62.35 g/m^2 and a thickness of 336 μm.

B. Chemicals

We employed various chemicals as repellent agents. Technical grade (93 %) betulin (Bt), with a molecular weight of 456.7 g/mol, was purchased from Innomost Oy in Finland. Reagent grade (95 %) stearic acid (SA), beeswax (BW) (CAS:8012–89–3), and ethyl cellulose (EC) (CAS: 9004–57–3) were all purchased from Sigma-Aldrich in Finland. Alkyl ketene dimer-based hydrophobizing agents (AKD) were provided by Kemira in Finland. Additionally, ethanol with a purity of 99.5 % and isopropanol were used as solvents in our experiments. All chemicals were used as received.

2.2. Methods

A. Solution preparation

Bt, SA, and EC were separately dissolved in ethanol at a temperature of 50 °C, with continuous magnet stirring at an apparent mixing speed of 1100 rpm for one hour. BW was dissolved in isopropanol under the same conditions. For SA and Bt solutions, varying concentrations, ranging from 5 to 25 g/L, were used. 25 g/L of a mixture of SA and EC (35:65 *w/w*) and a mixture of Bt and EC (35:65

w/w) were both dissolved in ethanol, separately. The received AKD solution was not diluted. Initially, different experimental sets went into effect to conduct the analysis and the screening led us to do the analysis at the same concentrations (20 g/L). However, in the case of samples coated with SA and Bt, based on insights from prior research [29–31], efforts have been undertaken to explore the possibility of achieving a WCA result equivalent to NW1-AKD (benchmarked sample) at lower concentrations as shown in Table 1

B. Application of biobased repellent solutions

Solutions were applied to the nonwoven substrates using a dip-coating method, involving five dip-and-dry cycles. The substrate was immersed in the coating solution for 1 minute and dried at 60℃ for 5 minutes. This process was repeated 5 times to prepare each sample. After the dip-and-dry cycles, the samples were cured for 20 minutes at 60℃.

C. Evaluation of properties

i. Water contact angle (WCA)

The WCA of fabrics was determined by using a sessile drop test employing the Theta Flex optical tensiometer from Biolin Scientific. A 5 μL drop of Milli-Q water was placed on the treated samples using an automatic dispenser and the contact phenomenon for 30 sec was measured at a camera angle set on the equipment for optimal image recording. The WCA was analyzed using OneAttension software which has a default analysis recipe for each measurement. The provided values represent an average of 10 measurements for each sample.

ii. Surface morphology

The surface morphology was assessed by scanning electron microscope (SEM) Zeiss Sigma VP. Samples were placed on top of a sample holder using carbon tape and coated by 80Au/20 Pd for about 40 sec at 20 mA using sputter coater type Q 150 R supplied by Quorum Technologies Ltd. Scanning electron microscope images were then taken using a Zeiss Sigma VP connected to a secondary electron detector with an acceleration voltage of 1.3−3 keV.

iii. Fourier Transform Infrared (FTIR) Analysis

The surface features of pristine and dip-coated nonwovens were examined in the solid state using an FTIR Spectrometer (PerkinElmer, USA) with the Attenuated Total Reflection head (FTIR-ATR). Measurements were carried out at room temperature with a $LiTaO_3$ MIR (Mid-infrared) detector with a signal-to-noise ratio (SNR) of 9.300:1. The spectra were recorded from 4000 cm^{-1} to 500 cm^{-1}, with a resolution of 4 cm^{-1}.

iv. Assessment of fabric structural parameters and weight gain

The fabric's structural parameters such as thickness, pore size diameter, and basis weight were measured before and after the hydrophobization treatments. The assessment of thickness was carried out according to ISO5084 with the Lorentzen and Wettre SE250D thickness tester micrometer. Thickness data was collected with a sample size of 10 points per sample.

The areal density (AD) of the sample is measured and expressed in grams per square meter (g/m^2). The method for obtaining this value is implicit, involving the simple process of weighing a known area and subsequently dividing the weight by the measured area. After the sample of known area was cut and conditioned at 65 ± 2 % RH and 25 ± 2°C for at least 24 hours, an analytical balance accurate to 1 mg was used to measure the mass of the sample. The mass was measured in triplicate and the average was used to calculate the areal density. The weight gain of the treated samples was measured in terms of add-on percentage. The formula in Eq. 1 was used to calculate weight gain.

$$\text{Weight gain}(\%) = \frac{\textit{Final AD} - \textit{Base AD}}{\textit{Base AD}} \times 100 \quad (1)$$

The pore size diameter of the treated and untreated samples was measured using a capillary flow porometer (Anton Paar Porometer 3 G Micro). A fabric sample with 25 mm diameter was prepared and placed in the sample holder on top of which an O-ring secures the measured sample area (20 mm diameter). The sample is then wetted with porofil and the porometer is sealed. The cumulative and differential flow of air was utilized to measure the pore size diameter, particularly in response to the intrusion of a porofil liquid in both wet and dry states. The average of the three replicates for the maximum, average, and minimum pore size measurements was reported in terms of mm.

For visual assessment of the porosity, light was emitted from one side of the sample and the openings were visualized using Olympus BX53M light microscope.

v. Tensile strength

ISO 9073–18 test standard was followed to test the tensile strength of the fabric samples using the Universal Tester Instron 4204. The fabric extension method was used with a 1 kN load cell and 5 mm/min extension rate. Samples were prepared with a specimen preparation template. Any breaks that occur within 5 mm of the jaws or at loads substantially less than the average that gave outliers were rejected. All values are an average of at least five samples.

Table 1
Sample recipe preparations and respective sample codes.

Nonwoven	Hydrophobic agents	Recipe (g/L)	Sample code
NW1	None	N/A	NW1
	Stearic acid (SA)	5	NW1-SA_5
		10	NW1-SA_{10}
		15	NW1-SA_{15}
		20	NW1-SA_{20}
		25	NW1-SA_{25}
	Betulin (Bt)	5	NW1-Bt_5
		10	NW1-Bt_{10}
		15	NW1-Bt_{15}
		20	NW1-Bt_{20}
	Ethyl cellulose (EC)	20	NW1-EC
	Beeswax (BW)	20	NW1-BW
	AKD solutions	As received	NW1-AKD
	EC + SA	25	NW1-EC+SA
	EC + Bt	25	NW1-EC+Bt
NW2	None	N/A	NW2
	SA	20	NW2-SA_{20}
	Bt	20	NW2-Bt_{20}
	EC + SA	25	NW2-EC+ES
	EC + Bt	25	NW2-EC+Bt
	AKD solutions	As received	NW2-AKD
NW3	None	N/A	NW3
	EC + SA	25	NW3-EC+SA
	EC + Bt	25	NW3-EC+Bt
	AKD solutions	As received	NW2-AKD

3. Results and discussion

3.1. Characterization of coated nonwovens

Table 2 shows the changes in thickness, pore size diameter (minimum, average, and maximum), basis weight, and weight gain for the nonwovens both before and after undergoing the hydrophobization treatment compared with the benchmarked sample. Nonwoven materials are characterized by their delicate nature and textured surfaces, which contribute to their intricate structural attributes. These qualities are instrumental in determining the performance and visual appeal of the final products. In various industrial applications, precise control over thickness, weight, and pore size diameter within predefined limits is essential.

In dip-coating for hydrophobic finishing, thickness and weight are closely correlated, indicating the effectiveness of the fabric in repelling water by forming an invisible shield. The coating weight represents the

Table 2
Structural parameters and add-on percentage of controlled and treated samples.

Samples	Thickness (μm)	Pore size diameter (μm)			Areal density (AD) (g/m^2)	Weight gain (%)
		Minimum	Mean	Maximum		
NW1	224 ± 2.54	10.27 ± 0.64	25.26 ± 0.15	31.31 ± 0.00	51. 56 ± 0.01	NA
NW1-SA20	335 ± 8.53	9.17 ± 1.06	17.75 ± 0.51	23.15 ± 2.16	91.95 ± 0.01	78.35
NW1-Bt20	247 ± 2.52	13.03 ± 2.58	24. 18 ± 0.62	29.61 ± 0.54	77.18 ± 0.01	49.67
NW1-EC	443 ± 4.74	15.29 ± 0.38	27. 87 ± 0.18	32.00 ± 0.00	86.19 ± 0.01	67.18
NW1-BW	264 ± 1.58	13.10 ± 1.07	26. 56 ± 0.84	32.31 ± 0.99	72.09 ± 0.01	39.84
NW1-EC+SA	390 ± 3.16	15.97 ± 2.27	27. 89 ± 0.47	33.25 ± 0.52	72.41 ± 0.01	40.43
NW1-EC+Bt	424 ± 4.11	16.93 ± 2.96	29.01 ± 0.51	33.01 ± 0.67	82.05 ± 0.02	59.13
NW1- AKD	397 ± 5.69	10.60 ± 0.60	20.38 ± 0.25	25.14 ± 0.53	99.45 ± 0.02	95.93
NW2	260 ± 4.11	35.09 ± 1.46	50.14 ± 1.97	58.45 ± 1.12	58.21 ± 0.01	NA
NW2-EC+SA	528 ± 6.64	28.29 ± 4.18	41.02 ± 2.93	47.20 ± 3.90	84.04 ± 0.03	44.37
NW2-EC+Bt	639 ±10.75	24.78 ± 2.99	43.62 ± 3.09	50.45 ± 1.20	88.49 ± 0.01	52.03
NW2-AKD	423 ± 5.44	24.88 ±2.58	38.35 ± 1.31	48.86 ± 2.55	106.10 ± 0.03	82.26
NW3	336 ± 5.05	31.67 ± 0.71	44.65 ± 0.26	52.28 ± 0.76	62.35 ± 0.02	NA
NW3-EC+SA	584 ± 8.22	25.15 ± 0.07	38.96 ± 0.94	41.49 ± 0.88	94.47 ± 0.05	51.51
NW3-EC+Bt	685 ± 9.17	27.22 ± 0.55	41.05 ± 0.77	44.51 ± 0.38	96.51 ± 0.03	54.79
NW3-AKD	514 ± 6.42	22.67 ± 2.32	35.11 ± 1.23	44.57 ±1.78	115.58 ± 0.02	83.37

applied hydrophobic substance, and careful control of both thickness and coating weight is essential for optimal water repellency without compromising other textile qualities.

As can be seen in Table 2, the hydrophobization treatments generally lead to an increase in the thickness and areal density (AD) of the nonwovens, primarily due to the incorporation of binders and hydrophobizing agents. Among the treated samples, NW1-Bt20 exhibited the least weight gain (49.67 %), contrasting with NW1-AKD, the benchmarked sample, which showed the highest weight gain at96 %. The variance in weight gain values of EC+Bt and EC+SA samples can be attributed to their porous structures and the degree of absorption of the hydrophobizing mixture.

As demonstrated in a recent study [32], a water-repellent agent, present in solid and granular forms, has been identified to significantly increase the weight and thickness of the treated substrate. The authors discovered that applying beeswax to cotton fabric led to a twofold increase in both weight and thickness.

The pore size distribution of nonwovens before and after hydrophobization treatment was reduced slightly (Table 2). This observation shows that despite the considerable weight gain and the presence of hydrophobizing agents on the nonwoven surfaces, the majority of pores remain open and accessible. The concentration of the coating solution and choice of solvent, were precisely controlled to avoid undesirable effects on the fiber and bond rotation in the nonwoven. The selection of crystallization conditions of agents, such as temperature of drying and solvent evaporation, also played a critical role in the formation and distribution of the coating. If these conditions are not thoroughly determined and controlled, it can result in pore blockage or uneven coating distribution, thereby affecting the porosity of the nonwoven. As the objective was to preserve the inherent pore size of the fabric as much as possible, with careful control of these parameters, we were able to ensure that the porosity of the fabric remained unaffected. In applications, such as filtration systems, pore size is critical to the separation efficiency and flux of the nonwoven material [33].

The pore size diameter of NW1 untreated and treated samples showed insignificant differences across all specimens except for NW1-SA20 and NW1-AKD. As shown in Figure S1 a, d, e, the effect of oblique illumination for NW1, NW1-EC, and NW1-BW looks similar. Some variations may arise due to the bond and fiber rotation of the nonwoven with the interaction of solvent during dipping and or very likely from the heterogeneity of the sample. The pores in NW1-SA20 and NW1-AKD appear darker compared to NW1 (Figure S1 a, b, f). Even though, the light illumination was taken at the same condition for all controlled and coated samples, the change in color difference for NW1-SA20 and NW1-AKD arises because of the blockage of light beam paths, resulting in a change in light permeability.

The application of a mixed formulation involving EC and SA or EC and Bt on to NW2 and NW3 resulted in the creation of a distinctive coating structure, as illustrated in the SEM micrographs (Fig. 2). This coating not only provided hydrophobicity on a highly porous substrate but also resulted in a modest reduction in pore size diameter as evidenced by Table 2 and visually observed in the oblique illumination images of the supporting Figure S1. The pristine NW2 and NW3, as well as their treated counterparts (NW2-EC+SA, NW2-EC+Bt, NW3-EC+SA, NW3-EC+Bt), are shown in the oblique illumination Figure S1(g-l) to demonstrate the effect of the coating process on pore size diameter. The observed reduction in pore size diameter suggests a significant influence stemming from the interaction of different chemicals within the coating formulation. This reduction can be attributed to interactions between EC and SA or Bt, resulting in a more compact arrangement of fibers and decreased pore size diameters.

3.2. *Surface morphology*

The surface morphology of the nonwovens before and after the hydrophobization treatments was investigated using SEM as shown in Figs. 1 and 2. NW1, an air-laid nonwoven depicted in Fig. 1a, exhibits randomly distributed cellulose fibers across its surface, alongside noticeable polymeric binder deposits at various locations. Coating NW1 with SA resulted in a

rough surface morphology comprised of micron-scale planar flakes as seen in Fig. 1e. With the increased concentration of SA, more flakes can be seen across the surface of NW1 in Fig. 1b-f. The presence of the flakes on the surface makes the surface rougher thereby increasing the hydrophobicity of NW1 as seen in Fig. 4a.

The morphology obtained by nonwovens treated with Bt solution was different from nonwovens treated by SA solution. NW1 treated with 20 g/L of Bt solution had flowery flakes that appeared on the surface as seen in Fig. 1j. These micro-flakes created a rough, spiky surface for NW1 thus inducing a very rough surface which caused a higher WCA for NW1 treated with Bt than SA solution.

Fig. 1 also shows the surface morphology of NW1 samples treated with EC, BW, and AKD. The presence of EC on fibers can be observed as some patches connecting fibers together. AKD, on the other hand, seems to have covered the surface of the NW entirely. The BW particles were not visible on the fiber surface (refer to Fig. 1l) due to the heat treatment

applied during fabric sample drying. Heating the fabric to 60 °C for 20 minutes causes the beeswax particles to melt and disperse across the

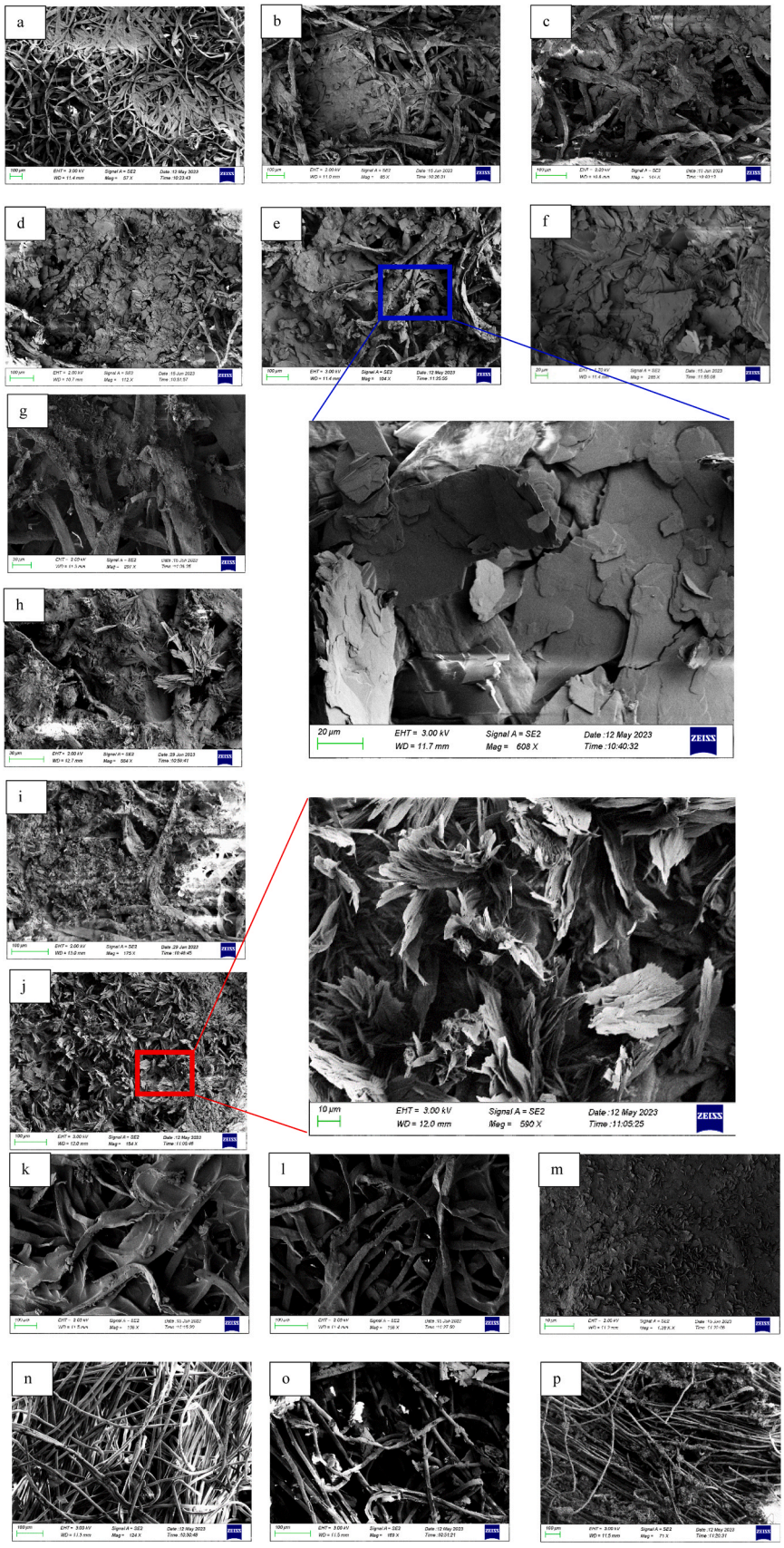

Fig. 1. SEM images of (a) NW1, (b) NW1-SA5, (c) NW1-SA10, (d) NW1-SA15, (e) NW1-SA20, (f) NW1-SA25, (g) NW1-Bt5, (h) NW1-Bt10, (i) NW1-Bt15, (j) NW1-Bt20, (k) NW1-EC, (l) NW1-BW, (m) NW1-AKD, (n) NW2, (o) NW2-SA20, (p) NW2-Bt20.

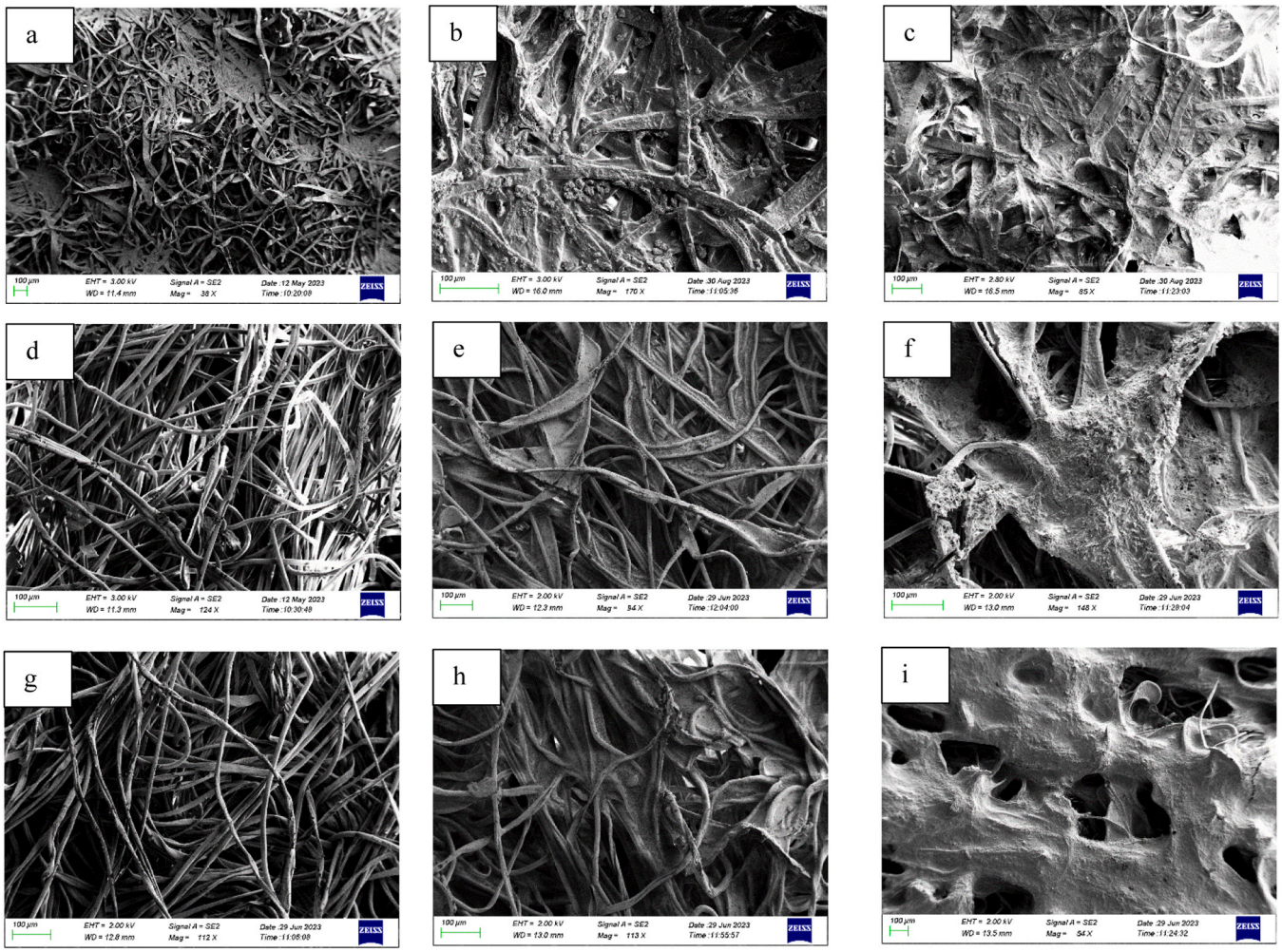

Fig. 2. SEM images of (a) NW1, (b) NW1-EC+SA, (c) NW1-EC+Bt, (d) NW2, (e) NW2-EC+SA, (f) NW2-EC+Bt, (g) NW3, (h) NW3-EC+SA, (i) NW3-EC+Bt.

fiber surface. As a result, the coating exhibits noticeably small, globular-shaped protrusions with micropores formed due to the vaporization of the solvent isopropanol in BW, a phenomenon observed in previous research as well [34].

NW2, consisting of lyocell fibers, and NW3, a blend of cotton and PLA, exhibiting distinct structures with longer, oriented fibers (Fig. 2d, g). The increased average pore size of NW2 and NW3, as previously discussed, was also confirmed by SEM. This structural difference led to a lower retention of SA or Bt particles on the surface of NW2, as depicted in Fig. 1o and p, respectively. As a result, a basic dip coating of NW2 and NW3 with the same solution fell short of achieving adequate coverage, likely due to (a) weak intermolecular interactions between hydrophobic particles and the surface and (b) higher porosity leading to reduced retention. To overcome this challenge, we introduced ethyl cellulose (EC) as a biobased binder to enhance the adhesion of Bt or SA particles to the nonwoven surface. The formulations of EC+SA create

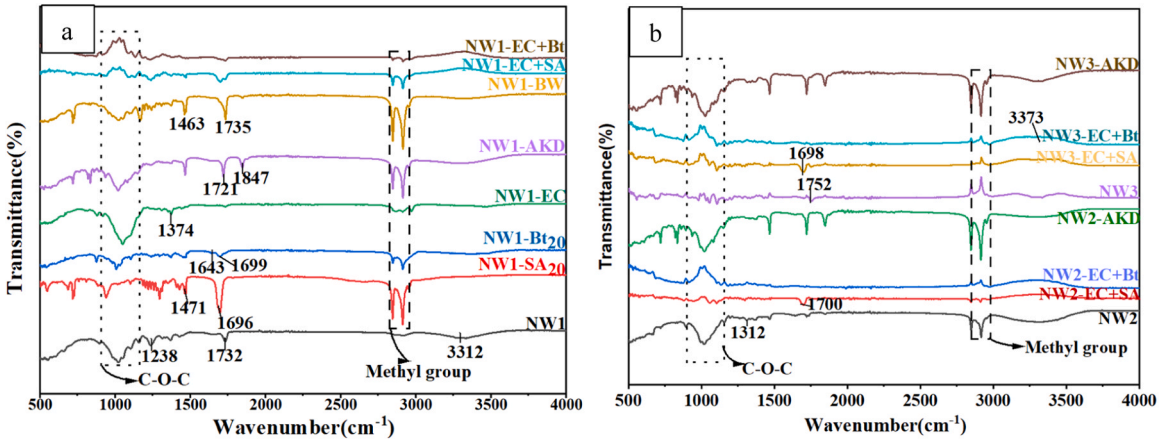

Fig. 3. Infrared spectra of coated and controlled samples of (a) NW1(b)NW2 and NW3.

microroughness on NW1 (refer to Fig. 2b) and nano-roughness on NW2 and NW3 (Fig. 2e, h). EC facilitates the binding and retention of surface modifying agents on the nonwoven. In EC+Bt mixtures, needle-like Bt emerges within the ethyl cellulose and extends outward, as depicted in Fig. 2c, f, i.

3.3. Analysis of FTIR results

The FTIR spectra of the coated and controlled samples of NW1, NW2, and NW3 are reported in Fig. 3. In the spectrum, a broad peak from 3200 to 3400 cm^{-1} is assigned to the stretching vibration of (-OH) in the cellulose fibers [35]. The intensity of these vibrations were reduced after coating using different hydrophobizing agents, indicating that the coating was bound to the surface of nonwovens [36]. The peaks from 2854 to 2926 cm^{-1} in the FTIR curve are associated with the presence of methyl groups [37]. The intensity at this peak is higher for SA, BW and AKD treated samples (Fig. 3a). However, the intensity of the methyl peak band around 2854–2926 cm^{-1} due to the vibrational mode of -CH_3 stretching bond in the NW2 and NW3 coated samples and in NW1-ES+SA and NW1-EC+Bt treated samples was relatively lower compared with treated samples of NW1, which suggests that SA, and Bt lies underneath EC (Fig. 2b, c). The presence of stearic acid in NW1-SA20 was evidenced by C═O stretching and CH_2 scissoring at 1696 and 1471 $cm^{-1,}$ respectively [38].

Betulin in NW1-Bt20 was identified by strong stretching of C═O that illustrates the conjugated bond from 1699 to 1700 cm^{-1} and C = C stretching at vibration 1643 cm^{-1} [39]. This peak's intensity of Bt in NW2 and NW3 was reduced due to the fact that the mix with EC reduces the intensity. The FTIR spectra of EC suggests shows an obvious asymmetric peak at roughly 2850–2950 cm^{-1}, which is related to single-bond CH stretching.

The distinctive peak at 1374 cm^{-1} has been attributed to single bond CH_3 bending and the increased intensity of the broad peak near 1100 cm^{-1}, caused by cyclic C-O-C stretching, indicates the deposition of EC on NW1-EC [40]. In contrast, these bands were not observed in NW2 and NW3 treated samples indicating the cleavage of EC because of the mix with Bt and SA. The strong bands at 2920 and 2850 cm^{-1} correspond to the stretching vibration of C–H in the methyl and methylene of AKD tails [41]. The characteristic bands at 1721 cm^{-1} and 1847 cm^{-1} connected to C═C and C═O lactone ring respectively was observed in NW1-AKD, NW2-AKD and NW3-AKD samples [41,42]. The distinctive peaks in the beeswax spectra were tied to C═O vibrations at 1163 cm^{-1}, C═O stretching at 1735 cm^{-1} and C-C stretching at 1463 cm^{-1} in NW1-BW [43].

To this end, it is possible to state that, FTIR indicates that finishes are structured similar that has anchor system-polymer-chain which allows for adhering to nonwovens and functional group that provides hydrophobicity via creating surface roughness or reducing surface tension.

3.4. Water contact angle (WCA)

The hydrophobicity assessment of NW1 samples treated with SA, involving concentrations ranging from 5 to 25 g/L, revealed a direct relationship between the solution concentration and the initial WCA as illustrated in Fig. 4a. The initial WCA increased from 101° at a concentration of 5 g/L to 129° at 20 g/L, and remained unchanged after 20 g/L. We also observed a gradual droplet penetration into the nonwovens treated with SA at concentrations below 20 g/L (Fig. 4b). Thus, achieving a consistently hydrophobic surface resistant to water droplet penetration required a minimum SA concentration of 20 g/L for NW1.

Stearic acid coating of the nonwoven plays on altering the surface roughness and surface tension of the substrate. On the one hand, the incorporation of the SA in or on the fiber and nonwoven surface, in the fiber pores, and in the spacing between the fibers in the structure of the nonwoven may makes that fabric hydrophobic because of the repellent layer formation that may arise from methyl group of SA (Fig. 3). The formation of a repellent film (Fig. 1e) up on evaporation of ethanol and subsequent anchoring of SA to polar fiber surfaces due to the polar–nonpolar junctions of methyl and carboxylic group of the repellent and hydroxyl group of the substrate, and or chemical reaction of the carboxylic and hydroxyl groups of the SA and the cellulose increases the water repellency of the coated sample. Coating also increases the surface roughness of the sample which enables to development a micro size air pockets structure that trapped air (water contact angle of air is assumed to be 180°) which repel the water increases the porosity and hydrophobicity as also found in [44,45].

The formation of micro-roughness on cellulosic textiles coated with stearic acid begins with the creation of nucleation sites, where molecules initially anchor to cellulose fibers. These nucleation sites serve as the foundation for further aggregation of stearic acid molecules, leading to the development of micro-scale peaks and valleys on the textile surface. This micro-rough texture enhances hydrophobicity by reducing the contact area for water and creating air pockets, which is confirmed from SEM images and contact angle measurements. This process significantly improves the water-repellent properties of the coated nonwovens [26,46]

As observed in prior literature [33], the SA lowers the surface free energy of the nonwoven, producing the water repellent effect observed. This reduces the attractive forces between water droplets and the substrate covered by SA (Fig. 4).

In the analysis of NW1 samples treated with Bt, it was observed that the concentration of Bt had a slightly lower effect on the initial WCA

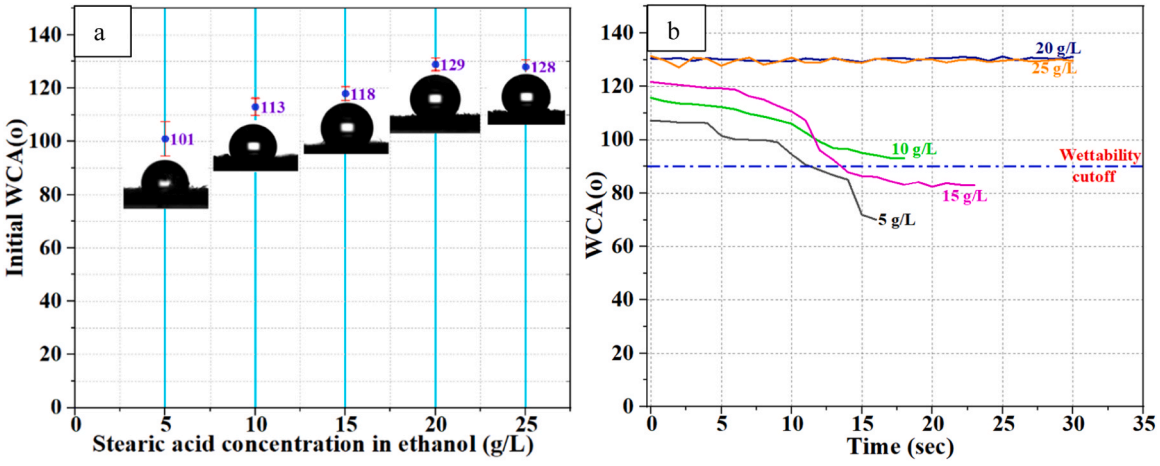

Fig. 4. (a) Initial WCA for NW1 treated with stearic acid at different concentrations (b) The variation of the WCA with time for NW1 treated with stearic acid.

compared with SA treated samples. The initial WCA exhibited a gradual increase from 118° at a concentration of 5 g/L to 134° at 20 g/L, as illustrated in Fig. 5. The increase in WCA continued with rising concentrations of the Bt solution. Even at the relatively lower concentration of 5 g/L, NW1-Bt demonstrated consistent hydrophobic properties, attributed to the naturally rough surface of the Bt treatment [31]. Similar to the SA crystallization mechanism, Bt recrystallizes onto the substrate's surface producing the micro-roughness-induced hydrophobicity observed [31]. The findings indicate that the presence of SA and Bt reduces the surface free energy of cellulosic nonwovens creating superhydrophobic interfaces [30,31].

When SA and Bt are coated on cellulose nonwoven, they create a monolayer or multilayer coating on the nonwoven that significantly reduces surface energy. This process involves several key mechanisms as explained in previous literature [47,48].

According to Fowkes's theory, the surface tension of liquids and surface free energy of solid surfaces can be considered to be consist of dispersion and polar components [49]. The extended Fowkes's equation (Eq. 2) breaks down the surface free energy (γ_{SG}) into several components, including dispersion (γ_{SG}^{d}), polar (γ_{SG}^{p}), hydrogen bonding (γ_{SG}^{H}), inductive forces ($\gamma_{SG}^{induction}$), acid-base interactions ($\gamma_{SG}^{acid-base}$), and other factors [50]:

$$\gamma_{SG} = \gamma_{SG}^{d} + \gamma_{SG}^{p} + \gamma_{SG}^{H} + \gamma_{SG}^{induction} + \gamma_{SG}^{acid-base} + \gamma_{SG}^{others} \quad (2)$$

When hydrophobic agents like SA and Bt are applied to cellulose nonwoven surfaces, their nonpolar hydrocarbon parts orient outward on the surface, which minimizes London dispersion forces and lowers the dispersion component. The hydrophobic coating also covers the cellulose's polar hydroxyl groups, drastically reducing the polar component (γ_{SG}^{p}) and preventing hydrogen bonding (γ_{SG}^{H}).

The Cassie–Baxter model (Eq. 3) explains how chemical surface heterogeneities, like the entrapment of air pockets between surface asperities, influence wettability. This model specifically addresses the impact of these surface variations on the overall surface behavior [51,52]:

$$Cos\theta_A = r \times f \times Cos\theta_Y - (1 - f) \quad (3)$$

where θ_A is the apparent/measured contact angle, θ_Y is the equilibrium Young's contact angle, r is the surface roughness, and f is the solid–liquid contact area fraction. The roughness factor is defined as the ratio of the actual surface area to the geometrically projected surface area. The occupation of a surface fraction $(1 - f)$ by air pockets augments the apparent contact angle.

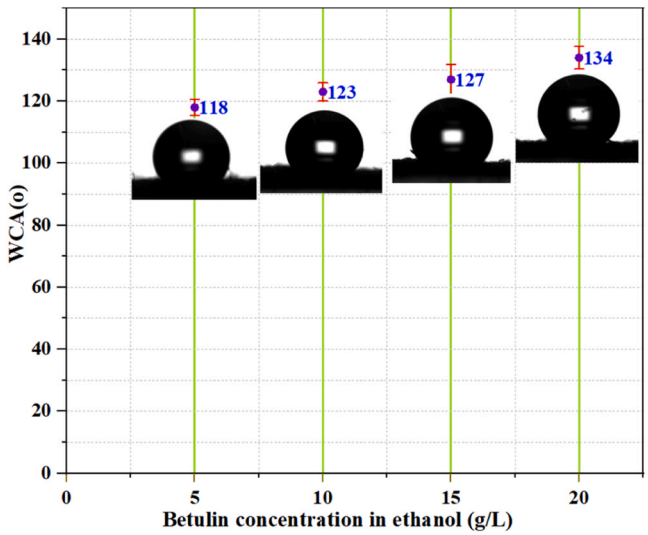

Fig. 5. WCA of NW1 samples treated with Bt at different concentrations.

In the context of surfaces coated with SA and Bt, the roughness introduced by these coatings (as shown in the SEM micrograph in Fig. 1) plays a crucial role in enhancing hydrophobicity. The increased roughness, represented by the roughness factor (r), reduces the effective contact area with water by creating more asperities where air can be trapped. This reduction in the solid–liquid contact area fraction (f) further augments the apparent contact angle (θ_A), making the surface even less wettable. Consequently, the combined effects of chemical surface heterogeneities and increased roughness contribute to a significant increase in hydrophobicity.

The combined effects of reduced polar interactions and hydrogen bonding along with increased surface roughness, are essential in creating hydrophobic surfaces on cellulosic nonwoven materials. This overall reduction in surface free energy is key to the hydrophobic properties of the coated nonwoven materials, making them significantly less likely to interact with water [46,53].

The degree of hydrophobization is linked to the chemical structure of the hydrophobizing agents, as well as the orientation and morphology of their particles on the nonwoven surface (Fig. 1). It should be noted that the adhesion of SA and Bt to cellulose fibers is relatively weak, governed by mild hydrophobic and van der Waals interactions. The adhesion of these hydrophobizing particles can be increased by adding binders.

Fig. 6 demonstrates a significant increase in hydrophobicity, reaching 119° and 113° for NW1-BW and NW1-EC samples, respectively. Despite the invisible surface roughness in these samples (Figs. 1k, 1l), the chemical composition of the agents likely plays a crucial role in imparting hydrophobicity to the treated substrate. The inclusion of BW introduces long fatty acid chains onto the nonwoven surface [54] leading to a decrease in surface free energy. Conversely, the hydrophobicity observed in EC-treated samples may stem from the inherent hydrophobic nature of EC [55] coupled with its film forming capacity.

NW2 and NW3 showed an open structure with sizable pores and higher thickness and weight compared with NW1. In addition to the main aim of investigating different biobased agents, we were interested in understanding how varying the structural characteristics of nonwoven materials influences their hydrophobic performance. Weight and thickness affect the surface structure, porosity, and absorption capacity of the nonwoven. Thicker and heavier materials absorb more hydrophobic coating into their structure, reducing the amount available on the surface, diminishing water repellency. Effective hydrophobicity relies on a continuous surface layer to repel water, and thicker materials may need more coating to maintain effective surface coverage and overall performance.

The distribution of coating material between the surface and bulk of the nonwoven also influences physio-mechanical properties. While bulk absorption can change strength and durability, it may compromise surface hydrophobicity. The balance between coating absorption and surface coverage determines hydrophobic efficiency. Hence, NW2 and NW3 were selected to see how varying pore sizes, weights, and thicknesses impacts the hydrophobic properties. These structural differences led to a lower deposition of coating agents on the nonwoven surface, as shown in Fig. 1o,p due to the increased absorption within the bulk of the material.

Despite being coated with either Bt or SA, NW2 and NW3 retained their hydrophilic nature due to the structural differences from NW1. The coating application resulted in only minimal adhesion of small flakes to the surface, falling short of attaining the intended level of hydrophobicity. Consequently, we decided to enhance the hydrophobization efficiency by introducing EC as a hydrophobic biobased binder. The treatment of NW2 and NW3 with a mixture of EC+SA or EC+Bt proved highly effective in enhancing hydrophobic properties, with WCA values exceeding 110°, as illustrated in Fig. 6. For benchmarking, we also applied the same formulation on NW1. The results demonstrated that the hydrophobicity achieved with the EC-based mix formulation on NW1 is higher than that of NW2 and NW3, showcasing that pore size diameter has a significant impact on the hydrophobicity of nonwovens.

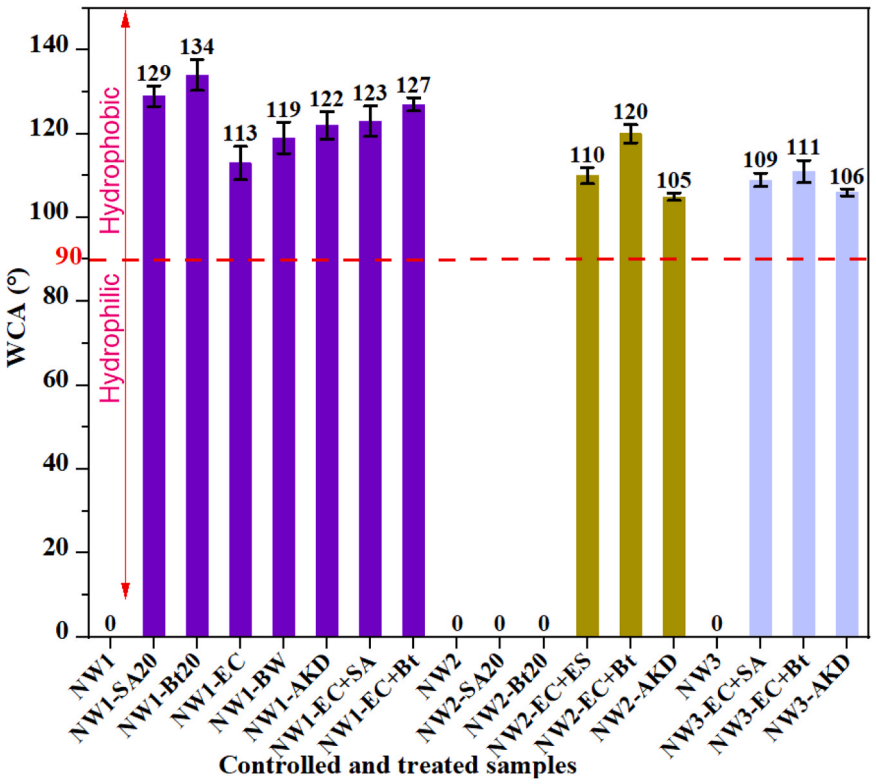

Fig. 6. Water contact angle of different samples.

This finding highlights the potential of hydrophobizing open fabric structures via tailored combinations of chemicals, with implications for diverse applications in enhancing the hydrophobicity of any fabric structures.

To summarize, enhanced hydrophobicity has been successfully attained on cellulosic nonwovens through the application of various biobased coating formulations. When applied to a porous and hydrophilic nonwoven substrate, these biobased coating formulations

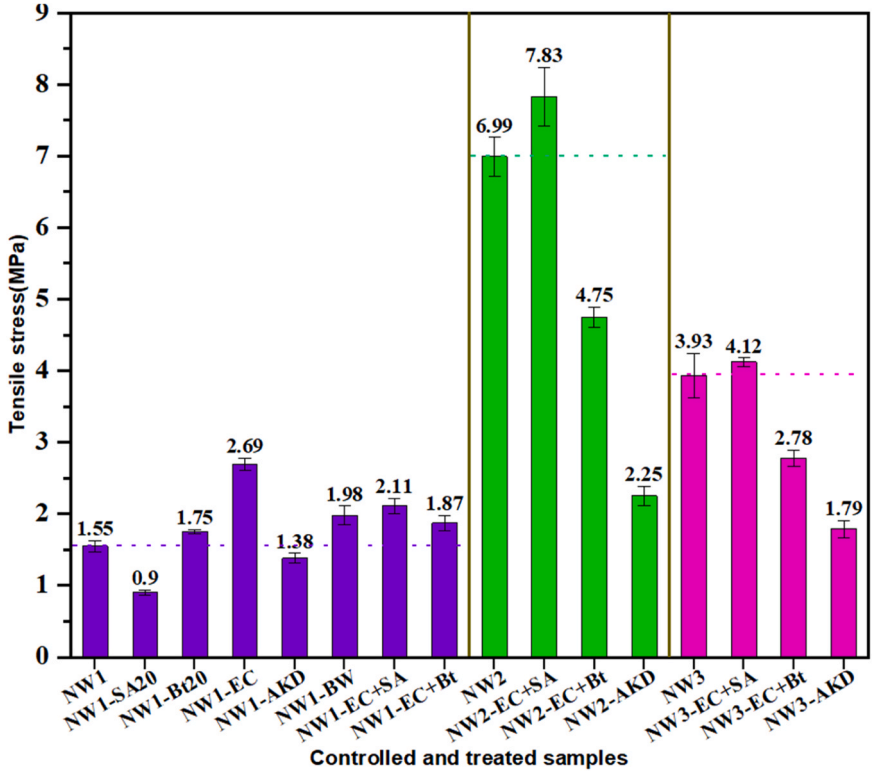

Fig. 7. The Effect of the treatment process on mechanical properties of nonwovens.

exhibited very good hydrophobic performance comparable to that achieved using AKD as our commercial benchmark.

3.5. Mechanical properties of treated samples

The structural composition and mechanical properties of cellulose-based nonwovens determine their versatility across various applications. For practical application consideration of the treated nonwoven, the mechanical properties after the treatment in machine direction were tested. NW1 has an ultimate tensile strength of 1.55 MPa, rendering it ideal for single-use applications like wiping, tabletop usage, and household cleaning. NW2 and NW3, with much higher ultimate tensile strengths of 6.99 MPa and 3.93 MPa, respectively, are suitable for specialized applications such as wet wipes and sanitary napkins. This variation in tensile strength aligns each nonwoven type with its designated application, showcasing the adaptability of cellulose-based nonwovens to meeting specific functional requirements.

Understanding how the various coatings impact the mechanical properties is an important factor to consider when determining the material's practical applications. The mechanical properties of NW1 treated with 20 g/L Bt, EC, and BW were increased with the ultimate strengths of 1.75 MPa, 2.69 MPa, and 1.98 MPa respectively. These treated samples had higher ultimate tensile strengths compared to the NW1 control sample (1.55 MPa). These additives had some flakes, particles, or film on the surface of the nonwoven, improving the mechanical properties of the nonwoven as seen in Fig. 7.

In the case of NW1 treated with SA, the strength of the nonwoven dropped by nearly 40 % to 0.902 MPa. It is crucial to point out that the integrity and strength of NW1, an air-laid nonwoven, primarily stem from the presence of the binder. The coating of NW1 with various hydrophobizing agents, such as SA, can impact its overall integrity due to the following factors: (a) the SA coating layer increases the thickness of the nonwoven and the cross-sectional area, which must withstand increased forces, leading to a general decrease in tensile strength, especially when the coating layer is weaker than the nonwoven substrate; (b) the application of an ethanolic SA solution on NW1 may diminish the adhesion of the binder to the fibers, alter the arrangement of cellulose fibers, and weaken the overall integrity of the nonwoven material; (c) the coating process has the potential to weaken inter-fiber bonds and introduce defects or irregularities, creating weak points that cause premature necking. These considerations highlight the complex interplay of factors influencing the mechanical properties of NW1 when subjected to hydrophobization treatments [22,27,56].

Contrary to the NW1 results, when EC+SA and EC+Bt mixtures were coated on NW2 and NW3, EC+SA increased the ultimate tensile strength while decreasing that of EC+Bt samples. Specifically, the average tensile strength for NW2-EC+SA and NW3-EC+SA was 7.83 and 4.12 MPa, respectively, compared to the controlled samples' tensile strength of 6.99 MPa for NW2 and 3.99 MPa for NW3. The lubricating effect of SA [57] coupled with its adherence to the nonwoven by EC may result in structural rearrangements contributing to the overall strength in enhancement in EC+SA samples.

However, mixing EC with Bt, and AKD formulations may reduce the friction between fibers, leading to a decrease in tensile strength observed in NW2-EC+Bt, NW2-AKD, NW3-EC+Bt, and NW3-AKD samples. Tensile stress on the other hand, is affected by coating thickness. The thickness of samples coated with a mixture of EC with Bt and AKD was considerably higher compared with other samples. This demonstrates that more coating materials that are not as strong as the fiber itself are added. As a result, when a similar force is applied to the same area, the stress may decrease simply because the area increases with materials that contribute less to the nonwoven strength.

In contrast to NW1, whose integrity relies on the presence of a binder, NW2 and NW3 are manufactured using hydroentanglement and needle punching techniques and are free from any binders. Consequently, the mechanical properties of NW2 and NW3 primarily stem from the mechanical interlocking of cellulose fibers, forming a cohesive structure.

It was surprising to observe a reduction in tensile strength after hydrophobization with EC+Bt and AKD, especially considering that NW2-EC+SA and NW3-EC+SA showed a slight increase in tensile strength (Fig. 7). The introduction of EC+Bt and AKD formulations appears to have interfered with the fiber cohesion causing the reduction in strength. Given that the exact chemical composition of AKD-based hydrophobizing agents is unknown, there is a possibility that the chemicals may form undesirable bonds with cellulose fibers or alter fiber-fiber bonding, compromising tensile strength. This aspect necessitates further investigation to understand the underlying mechanisms and optimize the hydrophobization process for these nonwoven materials.

4. Conclusion

The textile industry faces challenges in making cellulose hydrophobic due to regulatory issues [58,59]. The cellulosic nonwoven sector requires simple hydrophobization techniques that maintain sustainability and biodegradability [60] in an eco-friendly manner. The pollution caused by synthetic hydrophobic agents, due to their lack of biodegradability [61], highlights the need for biobased alternatives. These alternatives must be easy to apply, effective in small quantities, preserve structural and physicochemical properties [62], and meet environmental safety standards [59]. To aid in the design of eco-friendly material selection [63], a comparative study of biobased agents is essential for both academia and industry to understand their performance and effects on substrate properties.

This study comparatively analyzes the hydrophobic performance of various biobased agents and their impact on the physio-mechanical properties of nonwoven materials. The hydrophobizing finishes found to have an analogous configuration with an anchor system-polymer-chain that allows aggregation, adherence, or development of polar/non-polar junctions in and with the cellulosic nonwoven through solvent evaporation during drying and curing for adhering to nonwovens and a functional group that provides hydrophobicity. The formation of a rough, hierarchical surface and the low surface free energy of the compounds are crucial in enhancing hydrophobicity. Among the samples, NW1-Bt20 outperforms the other finishing agents, achieving a contact angle of 134°, with minimal impact on porosity and tensile strength. Additionally, combining ethyl cellulose (EC) with betulin (Bt) improves water contact angle (WCA) and offers better structural parameters compared to the EC-steaic acid formulation.

Future research should explore the application methods and technical properties of these biobased agents for specific uses such as face masks, medical aprons, surgical drapes, diapers, incontinence pads, food service tablecloths, and oil-absorbent pads in industrial settings. The techno-economics of these finishing agents should also be considered. As the industry seeks more sustainable and environmentally friendly solutions, further studies should focus on optimizing these formulations for large-scale applications and exploring the long-term environmental impacts of these substitutes.

Funding

This work was funded by Business Finland (SUSTAFIT, project number 211895).

CRediT authorship contribution statement

Ali Tehrani: Writing – review & editing, Supervision, Resources, Project administration, Investigation, Funding acquisition, Conceptualization. **Esubalew Gebeyehu:** Writing – review & editing, Writing – original draft, Methodology, Investigation, Formal analysis. **Ali Amin Tarhini:** Writing – review & editing, Supervision, Methodology,

Investigation.

Declaration of Competing Interest

The authors declare that they have no known competing financial interests or personal relationships that could have appeared to influence the work reported in this paper.

Data Availability

Data will be made available on request.

Acknowledgements

The authors express gratitude to SharpCell Oy and Suominen Oyj for supplying cellulose nonwovens, and to Kemira for providing the AKD-based hydrophobizing formulation. We also extend our gratitude to Marcus McDermott from Cornell University (USA) for his assistance with proofreading.

Conflicts of interest

The authors declare no conflict of interest.

Appendix A. Supporting information

Supplementary data associated with this article can be found in the online version at doi:10.1016/j.colsurfa.2024.135127.

References

[1] M.Z. Khan, J. Militky, M. Petru, B. Tomková, A. Ali, E. Tören, S. Perveen, Recent advances in superhydrophobic surfaces for practical applications: a review, Eur. Polym. J. (2022) 111481.
[2] L. Xing, Q. Zhou, G. Chen, G. Sun, T. Xing, Recent developments in preparation, properties, and applications of superhydrophobic textiles, Text. Res. J. (2022), 00405175221097716.
[3] R. Chapman, Applications of nonwovens in technical textiles, Elsevier, 2010.
[4] P.K. Saha, R. Mia, Y. Zhou, T. Ahmed, Functionalization of hydrophobic nonwoven cotton fabric for oil and water repellency, SN Appl. Sci. 3 (2021) 586.
[5] R. Sharif, M. Mohsin, S. Sardar, N. Ramzan, Z.A. Raza, Synthesis of nontoxic and bio based oil and water repellent polymers for cotton fabrics using stearic acid, succinic acid, and itaconic acid, J. Nat. Fibers 19 (2022) 12473–12485.
[6] S. Javaid, A. Mahmood, H. Nasir, M. Iqbal, N. Ahmed, N.M. Ahmad, Layer-by-layer self-assembled dip coating for antifouling functionalized finishing of cotton textile, Polymers 14 (2022) 2540.
[7] G. Liu, J. Wang, W. Wang, D. Yu, A novel PET fabric with durable anti-fouling performance for reusable and efficient oil-water separation, Colloids Surf. A: Physicochem. Eng. Asp. 583 (2019) 123941.
[8] A.P. Rananavare, J. Lee, Hydrophobic cotton fabric synthesized via dispersion polymerization from poly (glycidyl methacrylate) nanoparticles for self-cleaning applications, Prog. Org. Coat. 170 (2022) 107006.
[9] S. Sfameni, T. Lawnick, G. Rando, A. Visco, T. Textor, M.R. Plutino, Functional Silane-Based Nanohybrid Materials for the Development of Hydrophobic and Water-Based Stain Resistant Cotton Fabrics Coatings, Nanomaterials 12 (2022) 3404.
[10] D.W. Wei, H. Wei, A.C. Gauthier, J. Song, Y. Jin, H. Xiao, Superhydrophobic modification of cellulose and cotton textiles: Methodologies and applications, J. Bioresour. Bioprod. 5 (2020) 1–15.
[11] S. Barthwal, Y. Jeon, S.-H. Lim, Superhydrophobic sponge decorated with hydrophobic MOF-5 nanocoating for efficient oil-water separation and antibacterial applications, Sustain. Mater. Technol. 33 (2022) e00492.
[12] M. Diaa, A.G. Hassabo, Self-cleaning properties of cellulosic fabrics (a review), Biointerf. Res. Appl. Chem. 12 (2022) 1847–1855.
[13] S.R. Saad, N. Mahmed, M.M.A.B. Abdullah, A.V. Sandu, Self-Cleaning Technology in Fabric: A Review, IOP Conf. Ser.: Mater. Sci. Eng. 133 (2016) 012028.
[14] M. Yang, W. Liu, C. Jiang, Y. Xie, H. Shi, F. Zhang, Z. Wang, Facile construction of robust superhydrophobic cotton textiles for effective UV protection, self-cleaning and oil-water separation, Colloids Surf. A: Physicochem. Eng. Asp. 570 (2019) 172–181.
[15] S. Kim, Y. Cho, C.H. Park, Effect of cotton fabric properties on fiber release and marine biodegradation, Text. Res. J. (2022), 00405175211068781.
[16] I.S. Bayer, Superhydrophobic Coatings from Ecofriendly Materials and Processes: A Review, Adv. Mater. Interfaces 7 (2020) 2000095.
[17] W. Wang, L. Feng, B. Song, L. Wang, R. Shao, Y. Xia, D. Liu, T. Li, S. Liu, Z. Xu, Fabrication and application of superhydrophobic nonwovens: a review, Mater. Today Chem. 26 (2022) 101227.
[18] M. Farzam, M. Beitollahpoor, S.E. Solomon, H.S. Ashbaugh, N.S. Pesika, Advances in the fabrication and characterization of superhydrophobic surfaces inspired by the Lotus leaf, Biomimetics 7 (2022) 196.
[19] A.R. Tehrani-Bagha, Waterproof breathable layers–A review, Adv. Colloid Interface Sci. 268 (2019) 114–135.
[20] F. Mikaeili, P.I. Gouma, Super Water-Repellent Cellulose Acetate Mats, Sci. Rep. 8 (2018).
[21] G. Liu, P. Han, L. Chai, Z. Li, L. Zhou, Fabrication of cotton fabrics with both bright structural colors and strong hydrophobicity, Colloids Surf. A: Physicochem. Eng. Asp. 600 (2020) 124991.
[22] A.L. Mohamed, A.G. Hassabo, A.A. Nada, N.Y. Abou-Zeid, Properties of cellulosic fabrics treated by water-repellent emulsions, Indian J. Fibre Text. Res. (IJFTR) 42 (2017) 223–229.
[23] M. Abo-Shosha, Z. El-Hilw, A. Aly, A. Amr, A.S.I.E. Nagdy, Paraffin wax emulsion as water repellent for cotton/polyester blended fabric, J. Ind. Text. 37 (2008) 315–325.
[24] G. Lomax, Coated fabrics: part 1—lightweight breathable fabrics, J. Coat. Fabr. 15 (1985) 115–126.
[25] D.A. Holmes, Waterproof breathable fabrics, Handb. Tech. Text. 12 (2000) 282.
[26] T.A. Khattab, A.L. Mohamed, A.G. Hassabo, Development of durable superhydrophobic cotton fabrics coated with silicone/stearic acid using different cross-linkers, Mater. Chem. Phys. 249 (2020) 122981.
[27] R. Sharif, M. Mohsin, N. Ramzan, S.W. Ahmad, H.G. Qutab, Synthesis and application of fluorine-free environment-friendly stearic acid-based oil and water repellent for cotton fabric, J. Nat. Fibers 19 (2022) 1632–1647.
[28] Q. Li, Z. Fan, C. Chen, Z. Li, Water and oil repellent properties affected by the crystallinity of fluorocarbon chain in fluorine-silicon containing finishing agent, J. Text. Inst. (2019).
[29] Y. Wu, X.Y. Wu, F. Yang, J. Gan, H.L. Jia, The preparation of cotton fabric with super-hydrophobicity and antibacterial properties by the modification of the stearic acid, J. Appl. Polym. Sci. 138 (2021) 50717.
[30] M. Liu, C. Ma, D. Zhou, S. Chen, L. Zou, H. Wang, J. Wu, Hydrophobic, breathable cellulose nonwoven fabrics for disposable hygiene applications, Carbohydr. Polym. 288 (2022) 119367.
[31] T. Huang, D. Li, M. Ek, Water repellency improvement of cellulosic textile fibers by betulin and a betulin-based copolymer, Cellulose 25 (2018) 2115–2128.
[32] S. Kim, J.-E. Kim, D.-E. Song, S.-Y. Cho, Y. Hwang, Y. Chae, Effects of household water-repellent agents and number of coating layers on the physical properties of cotton woven fabrics, PLoS ONE 18 (2023) e0283261.
[33] J. Wu, W. Wei, S. Zhao, M. Sun, J. Wang, Fabrication of highly underwater oleophobic textiles through poly (vinyl alcohol) crosslinking for oil/water separation: the effect of surface wettability and textile type, J. Mater. Sci. 52 (2017) 1194–1202.
[34] J. Szulc, W. Machnowski, S. Kowalska, A. Jachowicz, T. Ruman, A. Steglinska, B. Gutarowska, Beeswax-modified textiles: method of preparation and assessment of antimicrobial properties, Polym. (Basel) (2020) 12.
[35] S. Ismaeilimoghadam, M. Sheikh, P. Taheri, S. Maleki, H. Resalati, M. Jonoobi, B. Azimi, S. Danti, Manufacturing of Fluff Pulp Using Different Pulp Sources and Bentonite on an Industrial Scale for Absorbent Hygienic Products, Molecules 27 (2022) 5022.
[36] E. Kasaw, A. Haile, M. Getnet, Conductive coatings of cotton fabric consisting of carbonized charcoal for E-Textile, Coatings 10 (2020) 579.
[37] D.C. Lingegowda, J.K. Kumar, A. Prasad, M. Zarei, S. Gopal, FTIR spectroscopic studies on cleome gynandra-Comparative analysis of functional group before and after extraction, Rom. J. Biophys. 22 (2012) 137–143.
[38] T.T. Nguyen, V.K. Nguyen, T.T.H. Pham, T.T. Pham, T.D. Nguyen, Effects of surface modification with stearic acid on the dispersion of some inorganic fillers in pe matrix, J. Compos. Sci. 5 (2021) 270.
[39] S. Cîntă-Pînzaru, C.A. Dehelean, C. Soica, M. Culea, F. Borcan, Evaluation and differentiation of the Betulaceae birch bark species and their bioactive triterpene content using analytical FT-vibrational spectroscopy and GC-MS, Chem. Cent. J. 6 (2012) 1–12.
[40] J. Desai, K. Alexander, A. Riga, Characterization of polymeric dispersions of dimenhydrinate in ethyl cellulose for controlled release, Int. J. Pharm. 308 (2006) 115–123.
[41] L. Li, M. Cao, J. Li, C. Wang, S. Li, Structure Optimization of Cellulose Nanofibers/Poly (Lactic Acid) Composites by the Sizing of AKD, Polymers 13 (2021) 4119.
[42] X. Song, F. Chen, F. Liu, Preparation and characterization of alkyl ketene dimer (AKD) modified cellulose composite membrane, Carbohydr. Polym. 88 (2012) 417–421.
[43] L. Svečnjak, G. Baranović, M. Vinceković, S. Prđun, D. Bubalo, I.T. Gajger, An approach for routine analytical detection of beeswax adulteration using FTIR-ATR spectroscopy, J. Apic. Sci. 59 (2015) 37–49.
[44] M. He, M. Xu, L. Zhang, Controllable stearic acid crystal induced high hydrophobicity on cellulose film surface, ACS Appl. Mater. Interfaces 5 (2013) 585–591.
[45] N. Garti, E. Wellner, S. Sarig, Effect of surfactants on crystal structure modification of stearic acid, J. Cryst. Growth 57 (1982) 577–584.
[46] S.-C. Shi, Y.-Q. Peng, Hydrophobicity and macroscale tribology behavior of stearic acid/hydroxypropyl methylcellulose dual-layer composite, Materials 14 (2021) 7707.
[47] P.C. Hiemenz, R. Rajagopalan, Principles of Colloid and Surface Chemistry, revised and expanded, CRC press, 2016.
[48] C.J. Van Oss, Interfacial forces in aqueous media, CRC press, 2006.
[49] F.M. Fowkes, Attractive Forces at Interfaces, Ind. Eng. Chem. 56 (1964) 40 (&).

[50] J.R. Chen, T. Wakida, Studies on the surface free energy and surface structure of PTFE film treated with low temperature plasma, J. Appl. Polym. Sci. 63 (1997) 1733–1739.
[51] P. Samyn, Wetting and hydrophobic modification of cellulose surfaces for paper applications, J. Mater. Sci. 48 (2013) 6455–6498.
[52] A.R. Tehrani-Bagha, Waterproof breathable layers - A review, Adv. Colloid Inter. 268 (2019) 114–135.
[53] X. Zhang, L. Wang, E. Levänen, Superhydrophobic surfaces for the reduction of bacterial adhesion, Rsc Adv. 3 (2013) 12003–12020.
[54] V.P.S. Muthukumaran, Experimental Research on the Water Repellency Property of Beeswax Treated and Bacterial Cellulosic Material, Int. J. Eng. Adv. Technol. (IJEAT) 8 (2019).
[55] Y.-H. Jiang, Y.-Q. Zhang, Z.-H. Wang, Q.-D. An, Z.-Y. Xiao, L.-P. Xiao, S.-R. Zhai, Cotton-derived green sustainable membrane with tailored wettability interface: Synergy of lignin and ethyl cellulose, Ind. Crops Prod. 183 (2022) 114993.
[56] U.M. Ekanayake, N. Rathuwadu, M.M. Mantilaka, R. Rajapakse, Fabrication of ZnO nanoarchitectured fluorine-free robust superhydrophobic and UV shielding polyester fabrics for umbrella canopies, RSC Adv. 8 (2018) 31406–31413.
[57] L. Zhang, S. Shakya, L. Wu, J. Wang, G. Jin, H. Sun, X. Yin, L. Sun, J. Zhang, Multi-dimensional visualization for the morphology of lubricant stearic acid particles and their distribution in tablets, Asian J. Pharm. Sci. 15 (2020) 60–68.
[58] X. Lim, Could the world go PFAS-free? Proposal to ban 'forever chemicals' fuels debate, Nature 620 (2023) 24–27.
[59] A.K. Patra, S.R.K. Pariti, Restricted substances for textiles, Text. Prog. 54 (2022) 1–101.
[60] S. Hartikainen, Biodegradability of Nonwoven Fabrics, BA thesis, Tampere University of Applied Sciences (2015).
[61] M.H. Whittaker, L. Heine, Toxicological and environmental issues associated with waterproofing and water repellent formulations. Waterproof and water repellent textiles and clothing, Elsevier, 2018, pp. 89–120.
[62] J. Bougourd, J. McCann, Designing waterproof and water repellent clothing for wearer comfort—A paradigm shift. Waterproof and water repellent textiles and clothing, Elsevier, 2018, pp. 301–345.
[63] H.Y. Erbil, Practical applications of superhydrophobic materials and coatings: problems and perspectives, Langmuir 36 (2020) 2493–2509.